Pure Appl. Geophys. 168 (2011), 2199–2210

DOI 10.1007/s00024-011-0265-7

Pure and Applied Geophysics

The Elastic Strain Energy of Damaged Solids with Applications to Non-Linear Deformation of Crystalline Rocks

Yariv Hamiel,[1] Vladimir Lyakhovsky,[1] and Yehuda Ben-Zion[2]

Abstract—Laboratory and field data indicate that rocks subjected to sufficiently high loads clearly deviate from linear behavior. Non-linear stress–strain relations can be approximated by including third and higher-order terms of the strain tensor in the elastic energy expression (e.g., the Murnaghan model). Such classical non-linear models are successful for calculating deformation of soft materials, for example graphite, but cannot explain with the same elastic moduli small and large non-linear deformation of stiff rocks, such as granite. The values of the third (higher-order) Murnaghan moduli estimated from acoustic experiments are one to two orders of magnitude above the values estimated from stress–strain relations in quasi-static rock-mechanics experiments. The Murnaghan model also fails to reproduce an abrupt change in the elastic moduli upon stress reversal from compression to tension, observed in laboratory experiments with rocks, concrete, and composite brittle material samples, and it predicts macroscopic failure at stress levels lower than observations associated with granite. An alternative energy function based on second-order dependency on the strain tensor, as in the Hookean framework, but with an additional non-analytical term, can account for the abrupt change in the effective elastic moduli upon stress reversal, and extended pre-yielding deformation regime with one set of elastic moduli. We show that the non-analytical second-order model is a generalization of other non-classical non-linear models, for example "bi-linear", "clapping non-linearity", and "unilateral damage" models. These models were designed to explain the abrupt changes of elastic moduli and non-linearity of stiff rocks under small strains. The present model produces dilation under shear loading and other non-linear deformation features of the stiff rocks mentioned above, and extends the results to account for gradual closure of an arbitrary distribution of initial cracks. The results provide a quantitative framework that can be used to model simultaneously, with a small number of coefficients, multiple observed aspects of non-linear deformation of stiff rocks. These include, in addition to the features mentioned above, stress-induced anisotropy and non-linear effects in resonance experiments with damaged materials.

Key words: Strain energy functions, nonlinearity, stress–strain relations, soft and stiff materials, damaged rocks, brittle deformation.

1. Introduction

Nonlinear elastic deformation of damaged rocks and other brittle materials is well-established by observations on different scales (Nishihara, 1957; Brace, 1965; Zoback and Byerlee, 1975; Brady, 1969; Schock, 1977; Ambartsumyan, 1982; Alm *et al*., 1985; Schmitt and Zoback, 1992; Johnson *et al*., 1996; Lockner and Stanchits, 2002; Bazaran and Nie, 2004). Distributed rock damage in the form of cracks, joints and other internal flaws develops as part of the rock formation and can increase significantly during tectonic loading. Several experimental studies under conditions of brittle deformation have revealed that the elastic properties strongly depend on the extent of the damage, leading to vanishing effective elastic moduli at large stresses just before failure (Lockner and Byerlee, 1980; Lockner *et al*., 1992; Hamiel *et al*., 2004).

The experimentally observed stress–strain curves are sometimes treated, all the way up to brittle instability, by use of linear elastic relations with effective moduli that depend on crack densities (O'Connell and Budiansky, 1974; Budiansky and O'Connell, 1976; Kachanov, 1992). This approach was successfully applied to synthetic materials with known internal structure and elastic properties of the matrix (Christensen, 1979; Rathore *et al*., 1995). The equivalent-linear approximation approach is the basis for many numerical codes (Bardet *et al.*, 2000; Assimaki and Kausel, 2002) for seismic site response that attempt to account for non-linear elasticity. Wu *et al.* (2009) reproduced temporal changes of the resonance frequency and motion amplification at a

[1] Geological Survey of Israel, 95501 Jerusalem, Israel. E-mail: yariv@gsi.gov.il
[2] Department of Earth Sciences, University of Southern California, Los Angeles, CA 90089-0740, USA.

site on the North Anatolian fault with damaged fault zone rocks using the equivalent linear approximation for sets of material properties at different times. However, high-resolution laboratory observations provide clear evidence of non-linear elastic behavior of damaged rocks (TenCate *et al.*, 2004; Pasqualini *et al.*, 2007).

In this paper we present observational and theoretical results on non-linear elastic (reversible) behavior of damaged solids, with a focus on the strain energy function of stiff crystalline rocks. In sect. "2" we review observations demonstrating non-linear elasticity in several contexts. In sect. "3" we discuss classical (analytical) and non-classical mathematical formulations for non-linear elastic models. In addition, we provide a theoretical basis for a general second-order non-linear expression for the elastic strain energy function of damaged solids. We discuss, in detail, properties of a non-classical formulation with a non-analytical term. The ability of the model to account simultaneously for multiple detailed experimental observations provides a strong test of its validity in describing realistic behavior of damaged crystalline rocks.

2. *Observations of Non-Linear Rock Deformation*

Nonlinear elastic behavior of damaged rocks is manifested at an early stage of deformation by stress-induced variations of the elastic wave velocities and anisotropy induced by non-hydrostatic load. These effects have been measured in the laboratory for many rock types starting with the pioneering work of Nur and Simmons (1969); Nur (1971), Bonner (1974), and more recent continuing studies (Sammonds *et al.*, 1989; Zamora and Poirier, 1990; Sayers *et al.*, 1990; Johnson and Rasolofosaon, 1996; Stanchits *et al.*, 2006; Hall, *et al.* 2008). These variations of rock properties are usually attributed to effects of micro-crack closure by the applied load, and thus depend on the crack density and applied stress level. Seismic wave anisotropy is also observed in the vicinity of large active fault zones and other environments with high rock damage (Crampin, 1987; Leary *et al.*, 1990; Miller and Savage, 2001; Peng and Ben-Zion, 2004; Liu *et al.*, 2005; Boness and Zoback, 2006). However, given the noisy environments near natural fault zones it is very challenging to establish direct connections between in-situ seismic wave anisotropy and variations of stress field in the crust (Karageorgi *et al.*, 1992).

Dynamic non-linear elastic behavior has been observed in a great variety of solids by elastic wave spectroscopy experiments (Johnson, 2006). Resonant bar experiments with rock samples show resonance curves with asymmetric shape and shifts of the spectral peak to lower frequencies with increasing loading, instead of the constant symmetric resonant frequency expected for linear media (Gordon, 1968; Winkler *et al.*, 1979; Johnson *et al.*, 1996; Smith and TenCate, 2000; Pasqualini *et al.*, 2007). The non-linear elastic properties of the examined materials are evaluated by measurements of the modulation of an ultrasonic wave by low-frequency vibration. Non-linear wave modulation spectroscopy has been suggested as an efficient tool for non-destructive damage detection and location (Solodov and Korshak, 2002; Pecorari and Solodov, 2006).

Nonlinear elasticity is also observed in seismic records of ground motion in sediments and highly-damaged fault zone rocks (Johnson *et al.*, 1996; Field *et al.*, 1997; Rubinstein and Beroza, 2004; Pavlenko and Irikura, 2003; Wu *et al.*, 2009). These observations usually focus on the non-linear behavior of wave resonance and spectrum. Comparison of seismograms from weak and strong earthquakes indicates that attenuation becomes non-linear at high amplitudes (Frankel *et al.*, 2002; Beresnev, 2002; Hatzell *et al.*, 2002, 2004; Bonilla *et al.*, 2005; Tsuda *et al.*, 2006; Sleep and Hagin, 2008).

Laboratory experiments on stress–strain relations indicate that the behavior of soft materials, for example graphite (Kaji *et al.*, 2001), sediments (Exadaktylos, 2006), and soils (Li and Ding, 2002), is strongly non-linear under stress substantially lower than the yielding level producing permanent inelastic deformation. In contrast, the behavior of stiff crystalline rocks is approximately linear up to the stress level corresponding to the onset of acoustic emission (AE) signifying brittle yielding. However, measurements of the volumetric deformation reveal significant dilation under shear loading before yielding in both soft (e.g., soil) and stiff (e.g., granite)

materials (Paterson, 1978; Schock and Louis, 1982; Lockner *et al*., 1992; Schmitt and Zoback, 1992). Dilatancy was first scientifically described by Reynolds in 1885, who coined the term, and is assumed to be associated with opening and closure of micro-cracks. Walsh (1965) suggested that this feature should lead to an increase of Young's modulus of a cracked solid under compression and a decrease under tension. The closure of micro-cracks in rocks under compressive stress was directly observed in laboratory experiments by Batzle *et al*. (1980), who also reported strongly non-linear behavior in hydrostatic stress–strain measurements. Rock dilation and related pore pressure changes under undrained conditions have been observed in more recent experiments of Lockner and Stanchits (2002).

Several studies have revealed that the values of the elastic moduli abruptly change when the loading reverses from compression to tension. For example, Young's modulus of graphite is 20% less under tension than it is under compression (Jones, 1977), the difference between the tensile and compressive Young's moduli for different types of iron is up to 30%, and the compressive modulus for concrete (Ambartsumyan, 1982) may be up to three times larger than the tensile value. Rock-mechanics experiments in which beams of Indiana limestone were deformed under four-point loading provided, simultaneously, significantly different apparent tensile and compressive moduli for small strains (Weinberger *et al*., 1994). Results of Basaran and Nie (2004) from strain-controlled tension–compression uniaxial tests with a composite brittle material (lightly cross-linked polymethyl methacrylate filled with alumina trihydrate) revealed a clear correlation between increasing crack density and decreasing stiffness.

3. Theory and Experimental Verification

In this section we discuss theoretical results on hyperelastic constitutive models for which non-linear stress–strain relations are derived from strain energy functions (Ogden, 1984). The energy potential of an isotropic elastic solid per unit volume, U, is a function of three invariants of the strain tensor ε_{ij} (Truesdell and Noll, 2004), which for small deformation are $I_1 = \varepsilon_{kk}$, $I_2 = \varepsilon_{ij}\varepsilon_{ij}$ and $I_3 = \det(\varepsilon_{ij})$. The stress–strain relations are obtained as a derivative of the energy function with respect to the strain tensor:

$$\sigma_{ij} = \frac{\partial U(I_1, I_2, I_3)}{\partial \varepsilon_{ij}} \tag{1}$$

The basic assumption of classical theories is that the energy function is analytical and thus a polynomial of the strain invariants. Non-classical non-linear models drop the assumption of analyticity and consider more general functions of strain invariants.

As already mentioned, our focus is on brittle deformation of stiff and dense crystalline rocks. We consider specifically a non-classical second-order function of the strain invariants in which a non-analytical term leads to a "kink" in the stress–strain relation that is attributed to crack opening and closure. Below we compare predictions of the classical Murnaghan (1951) framework and the examined non-classical model with results of dynamic and quasi-static experiments with westerly granite samples. This rock type was used extensively in laboratory experiments because it is a representative example of low-porosity crystalline rock in the Earth's crust.

3.1. Classical Non-Linearity: Murnaghan Model

Murnaghan (1951) provided a non-linear analytical expression for the strain energy in the form:

$$U = \frac{\lambda}{2} I_1^2 + \mu I_2 + A I_1^3 + B I_1^3 + B I_1 I_2 + C I_3 + \ldots, \tag{2}$$

where λ and μ are Lame constants associated with the second-order Hookean terms, and A, B, and C are additional elastic moduli of the third-order terms. Substituting Eq. (2) into Eq. (1) leads to stress–strain relations that include both linear (Hookean) terms and second-order (quadratic) terms. Models with high-order terms can be successful in large-strain analysis of the Earth's interior (Birch, 1952) or in reproducing the non-linear stress–strain relations of soft materials, like sediments (Exadaktylos 2006) or graphite (Kaji *et al*., 2001). Hughes and Kelly (1953) provided analytical expressions for the associated elastic wave velocities, including their change with

applied load and stress-induced seismic wave anisotropy. JOHNSON and RASOLOFOSAON (1996) used the MURNAGHAN (1951) model to describe observed stress-induced effects on waves during experiments with Barre Granite (NUR and SIMMONS, 1969) and other types of rocks. They found that the non-Hookean moduli in the Murnaghan model (2) that best describe the observed stress-induced anisotropy of the Barre granite sample are approximately three orders of magnitude larger than the Hookean constants. This implies significant deviation from linear (Hookean) stress–strain relations at very small strains of the order of 10^{-3}. However, this expectation is not compatible with rock mechanics experiments with stiff granite samples.

REINER (1945) presented a mathematical theory of dilatancy using the Murnaghan elastic energy (Eq. 2) and demonstrated that dilatancy is associated with third-order terms. SCHOCK and LOUIS (1982) conducted proportional loading experiments with Westerly granite samples in which the ratio between the stress components (σ_3/σ_1) was kept constant. Figure 1 shows mean stress versus volumetric strain measured during these experiments. In each test (σ_3/σ_1) was kept constant, where $\sigma_3/\sigma_1 = 0$ corresponds to uniaxial loading and $\sigma_3/\sigma_1 = -2$ corresponds to pure shear. The observed deformation in the vicinity of the pure shear conditions, $\sigma_3/\sigma_1 = -2.1$ and -1.58, implies dilatancy of the granite samples. These experimental results demonstrate that linear elasticity fails to describe Westerly granite deformation even under small stresses, and highlight the need for non-linear elastic model. As shown in Fig. 1a, the Murnaghan model provides a reasonable fit to the experimental data for all types of loadings, and it explains the dilation of granite when shear stress is applied. The elastic moduli that were used to fit the data are $\lambda = \mu = 1.3 \times 10^4$ MPa for Lame constants and $A = 1.1 \times 10^6$ MPa, $B = -6.7 \times 10^6$ MPa, and $C = -6.6 \times 10^6$ MPa for the Murnaghan constants. These values were taken from stress-induced anisotropy experiments with Barre granite samples (JOHNSON and RASOLOFOSAON, 1996). Thus, using similar values of the elastic moduli for granite samples, the Murnaghan model can explain both stress-induced seismic wave anisotropy (JOHNSON and RASOLOFOSAON, 1996) and deviations from linear stress–strain relations under relatively low stresses in granite samples (Fig. 1a). However, as shown next, using the same set of elastic moduli, the Murnaghan model cannot be extended to higher stress values.

Figure 2 presents a comparison between experimental results of triaxial loading under 50 MPa confining pressure with a G3 Westerly granite sample (LOCKNER *et al.*, 1992) and calculated stress–strain relations (red lines). Figure 2a shows the calculated differential stress versus axial and transversal strains using the Murnaghan model with the same set of moduli as estimated above and presented in Fig. 1a. During the G3 experiment an abrupt increase in AE, corresponding to initiation of fracturing, was recorded near 250 MPa differential stress. This

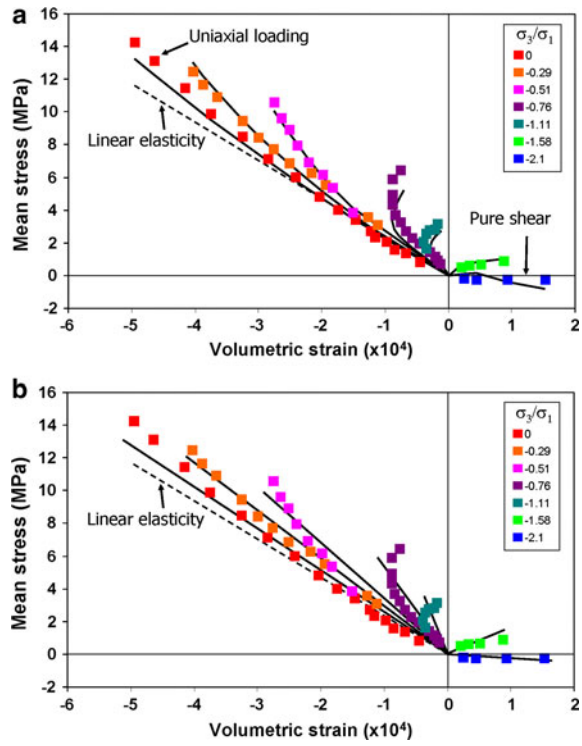

Figure 1
Measured mean stress versus volumetric strain for proportional loading experiments with Westerly granite compared with calculated curves. During each experiment the ratio between the stress components (σ_3/σ_1) was kept constant. *Symbols* indicate experimental results from SCHOCK and LOUIS (1982). **a** Calculated mean stress and volumetric strain curves using the Murnaghan model (Eq. 2). The elastic moduli are: $\lambda = \mu = 1.3 \times 10^4$ MPa, $A = 1.1 \times 10^6$ MPa, $B = -6.7 \times 10^6$ MPa, and $C = -6.6 \times 10^6$ MPa. **b** Calculated mean stress and volumetric strain curves using our non-classical second-order model (Eqs. 4, 5). The elastic moduli are $\lambda = \mu = 1.3 \times 10^4$ MPa and $\gamma = 0.3\lambda$

implies that granite samples may be loaded up to relatively high stresses without significant damage increase. It also implies that the same elastic properties should be expected until about 250 MPa differential stress. Figure 2a indicates that the Murnaghan model cannot explain the elastic deformation of granite samples under relatively large stresses. Because some of the third-order Murnaghan moduli are negative, the slope of the simulated stress–strain curve becomes negative at about 50 MPa differential stress. This means that the Murnahgan model predicts macroscopic failure of the sample at about 50 MPa, well below the observed strength of the granite, and also well below the onset of AE or damage accumulation at about 240 MPa. On the basis of these results it seems that Murnaghan model is unable to describe deformation of stiff crystalline rocks under both small and large stresses with the same elastic moduli.

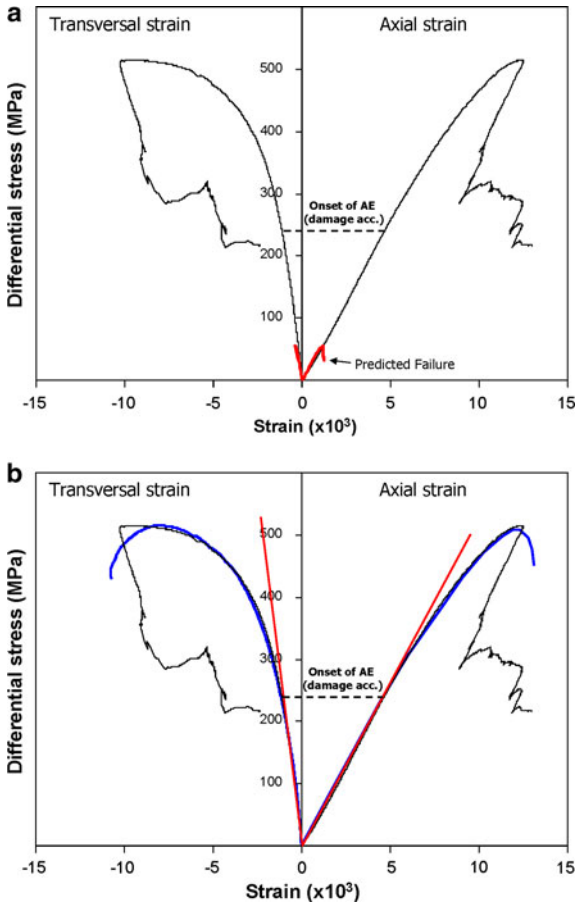

Figure 2
Measured axial and transversal components of stress versus strain (*black lines*) for the G3 Westerly granite triaxial experiment (Lockner *et al.*, 1992) compared with calculated curves. **a** Calculated stress–strain curves (*red line*) using the Murnaghan model (Eq. 2). The elastic moduli are $\lambda = \mu = 1.3 \times 10^4$ MPa, $A = 1.1 \times 10^6$ MPa, $B = -6.7 \times 10^6$ MPa, and $C = -6.6 \times 10^6$ MPa. **b** Calculated stress–strain curves using our model (Eqs. 4, 5). The red line shows calculations with constant elastic moduli: $\lambda = \mu = 1.3 \times 10^4$ MPa and $\gamma = 0.3\lambda$. The *blue line* shows calculations with the same initial elastic moduli that also account for damage accumulation and rigidity reduction after the onset of damage (Hamiel *et al.*, 2004)

3.2. Non-Classical Non-Linearity

For many brittle materials the elastic properties are highly sensitive to the sense of loading (tension or compression). This feature may be associated with micro-cracks closure under compression and opening under tension. This provides a physical basis for non-classical non-linear models with elastic moduli that depend on the type of loading. Analyzing non-linear wave modulation spectroscopy experiments, Pecorari and Solodov (2006) suggested a 1D "clapping" model with different elastic moduli for tension and compression:

$$\sigma = E_0\left(1 - H(\varepsilon)\left(\frac{\Delta E}{E_0}\right)\right)\varepsilon, \tag{3}$$

where $H(\varepsilon)$ is the Heaviside step function; E_0 is the elastic modulus under compression, and ΔE is its change under stress reversal to tension. They showed that experimentally observed modulation of higher harmonic spectra may be well reproduced with this model. A more complicated "unilateral" damage model (Chaboche, 1992; Lamaitre and Desmorat, 2005) that describes the material elastic behavior only in the principal axes also assumes different elastic moduli for tension and compression.

A 3D non-classical non-linear model was suggested by Lyakhovsky and Myasnikov (1984) on the basis of a micro-mechanical model with non-interacting randomly oriented cracks embedded inside a homogeneous elastic matrix. According to this model the elastic energy is written as:

$$U = \frac{\lambda}{2}I_1^2 + \mu I_2 - \gamma I_1\sqrt{I_2}. \tag{4}$$

The elastic energy (Eq. 4) includes a third non-Hookean second-order term with modulus γ that

couples volumetric and shear strain. The solution may be derived using the effective medium theory of Budiansky and O'Connell (1976) for non-interacting cracks that dilate and contract in response to tension and compression (Lyakhovsky *et al.*, 1997), or by expanding the strain energy potential as a general second-order function of I_1 and I_2 and eliminating non-physical terms (Ben-Zion and Lyakhovsky, 2006). Energy expressions with non-integer power of state variables are common for other non-linear systems, for example Hertzian theory for elastic deformation of a granular media and Van der Waals energy equation for a non-ideal gas. Using Eq. (1), the stress–strain relation associated with the strain energy function (Eq. 4) is:

$$\sigma_{ij} = \left(\lambda I_1 - \gamma\sqrt{I_2}\right)\delta_{ij} + \left(2\mu - \gamma\frac{I_1}{\sqrt{I_2}}\right)\varepsilon_{ij}, \qquad (5)$$

where δ_{ij} is the Kronecker delta. Equation (5) reduces to the linear stress–strain relations for an undamaged solid with $\gamma = 0$.

The stress–strain relations (Eq. 5) might be re-written in a Hookean form with effective elastic moduli:

$$\begin{aligned} \sigma_{ij} &= \lambda_{eff} I_1 \delta_{ij} + 2\mu_{eff}\varepsilon_{ij} \\ \lambda_{eff} &= \lambda - \frac{\gamma}{\xi} \\ \mu_{eff} &= \mu - \frac{1}{2}\gamma\xi, \end{aligned} \qquad (6)$$

where $\xi = I_1/\sqrt{I_2}$, referred to as the strain invariants ratio, ranges between $-\sqrt{3}$ for 3D compaction to $\sqrt{3}$ for 3D expansion, and is zero for pure shear or zero volumetric strain ($I_1 = 0$). The stress–strain relations (Eq. 6) imply that the effective moduli abruptly change upon stress reversal from tension to compression and remain constant under proportional loading with constant ξ. In this sense, the model is an extension of the non-classical models discussed earlier to a fully 3D framework. Equations (5) and (6) also account for material dilatancy. This may be demonstrated by substituting $\xi = 0$ into Eqs. (5) or (6) for pure shear or zero volumetric strain ($I_1 = 0$) and calculating the mean stress (trace of the stress tensor)

$$\sigma_{ii} = -3\gamma\sqrt{I_2}. \qquad (7)$$

The negative sign means that 3D compression should be applied to preserve zero expansion under shear; otherwise the material will expand under shear loading. Figure 1b demonstrates the relations between the calculated mean stress and volumetric strain (Eq. 5) for different proportional loadings, in comparison with the experimental results of Schock and Louis (1982) shown also in Fig. 1a. In these calculations we assume a Poisson ratio of 0.25 for the intact rock ($\lambda = \mu$), and fit the data by varying the γ value and searching for the best approximation. The moduli obtained by use of this procedure are: $\lambda = \mu = 1.3 \times 10^4$ MPa and $\gamma = 0.3\lambda$, corresponding to some initial damage of the rock sample. Note that the experimental results cannot be explained by linear elasticity, i.e., $\gamma = 0$ for damage-free intact rock (dashed line in Fig. 1). The different slopes of the stress–strain curves depending on the loading conditions represent reasonably well the general tendency of the experimental data. The deviation of the experimental points from the straight lines may be attributed to gradual crack closure under increasing pressure, as reported by Batzle *et al.* (1980), instead of the abrupt change under stress reversal assumed by Eqs. (5) and (6). This feature will be taken into account by an extended version of the model presented in the next section.

Figure 2b shows a comparison between calculated stress–strain relations (red lines) using the same set of values as in Fig. 1b ($\lambda = \mu = 1.3 \times 10^4$ MPa and $\gamma = 0.3\lambda$) and G3 experimental data (Lockner *et al.*, 1992). The calculated stress–strain values fit well the observed data over the range of loading from zero to the onset of AE or damage accumulation, where significant material weakening and irreversible deformation begin. As demonstrated by Hamiel *et al.* (2004), the entire curve up to macroscopic failure may be fitted by incorporating damage evolution to account for gradual changes of the elastic moduli following the onset of AE (blue line in Fig. 2b). However, the focus of this work is on reversible non-linear behavior even before damage accumulation, and therefore we limit our current analysis to calculations associated with fixed (constant) elastic moduli. Comparisons of the fits of Figs. 1b and 2b with those shown in Figs. 1a and 2a suggest that the presented non-analytical energy potential provides a better representation for the behavior of stiff crystalline rocks, over the range of loadings with fixed material damage, than the classical Murnaghan

model. However, it is important to examine if the non-analytical term of the elastic energy (Eq. 4) is unique, what is the general form of a second-order energy function, and how to account for gradual crack closure. These issues are discussed in the next section.

3.3. *General Form for the Second-Order Elastic Energy Function*

The only assumption made here is that the elastic energy is a second-order function of the strain tensor invariants. This implies that the energy may be written as:

$$U(\varepsilon_{ij}) = \varepsilon_{ij}\varepsilon_{ij} \cdot f\left(\frac{\varepsilon_{ij}}{\sqrt{\varepsilon_{ij}\varepsilon_{ij}}}\right) = I_2 \cdot f\left(\frac{\varepsilon_{ij}}{\sqrt{I_2}}\right), \qquad (8)$$

where $f(\bullet)$ is a general second-order function. The normalized strain tensor $\varepsilon_{ij}/\sqrt{I_2}$ $\left(\varepsilon_{ij}\varepsilon_{ij}/I_2 = 1\right)$ has only two strain invariants ξ and ζ (instead of three), corresponding to normalized I_1 and I_3 invariants:

$$\begin{aligned} \frac{\varepsilon_{kk}}{\sqrt{I_2}} &= \frac{I_1}{\sqrt{I_2}} \equiv \xi \\ \det\left(\frac{\varepsilon_{ij}}{\sqrt{I_2}}\right) &= \frac{I_3}{I_2\sqrt{I_2}} \equiv \zeta \end{aligned} \qquad (9)$$

Therefore, a general second-order strain energy function can be written as:

$$U(\varepsilon_{ij}) = I_2 \cdot f(\xi, \zeta) \qquad (10)$$

Lyakhovsky *et al.* (1997) and others demonstrated that the dependency of the elastic potential on the third strain invariant, I_3, is very weak and may be neglected. Hence, in such cases U can be written as:

$$U(\varepsilon_{ij}) = I_2 \cdot f(\xi). \qquad (11)$$

The elastic potential (Eq. 4) can now be obtained by using a polynomial function $f(\bullet)$ up to the second order:

$$f(\xi) = a_0 + a_1\xi + a_2\xi^2. \qquad (12)$$

Substituting Eq. (12) back into Eq. (11) leads to:

$$U(\varepsilon_{ij}) = a_0 I_2 + a_1 I_1\sqrt{I_2} + a_2 I_1^2, \qquad (13)$$

which differs from Eq. (4) only in notation for the coefficients and order of the terms. These results provide guidance on how the general form of a second-order energy function could be constructed, and demonstrate that the functional form (Eq. 4) is equivalent to Taylor expansion up to the second order of the function $f(\bullet)$ in Eq. (11).

The general expression (Eq. 11) of the energy as a function of I_2 and ξ predicts, as discussed earlier, that the effective elastic moduli remain constant under proportional load and abruptly change on reversal of the sense of the stress. In order to expand the formulation and account for a gradual crack closure, we return to simplified 1D bi-linear stress–strain relations with elastic moduli E, that change from $E + \gamma$ to $E - \gamma$:

$$\sigma = E\varepsilon - \gamma|\varepsilon|. \qquad (14)$$

With simple modification the abrupt change of the elastic moduli is shifted from the point $\varepsilon = 0$ to an arbitrary value $\varepsilon = \varepsilon_c$

$$\sigma = E\varepsilon - \gamma[|\varepsilon - \varepsilon_c| - \varepsilon_c]. \qquad (15)$$

This assumes that instead of crack closure at zero strain, it occurs at some compressive strain, ε_c. Introducing some weight function $w(\varepsilon_c)$ that represents the relative amount of micro-cracks that are closed at $\varepsilon = \varepsilon_c$, the stress–strain relations become:

$$\sigma = E\varepsilon - \gamma \int_{-\infty}^{\infty} w(\varepsilon_c)[|\varepsilon - \varepsilon_c| - \varepsilon_c]d\varepsilon_c \qquad (16)$$

If all the micro-cracks are closed when the strain becomes compressive, slightly more than $\varepsilon = 0$, and the weight function is equal to the delta-function, $w(\varepsilon_c) = \delta(\varepsilon_c)$, Eq. (16) reduces back to Eq. (14). Following these ideas we suggest modifying the non-analytical third term $I_1\sqrt{I_2}$ of the energy function (Eq. 4), and write the invariants of the strain tensor shifted by certain volumetric strain ε_c:

$$\begin{aligned} U = {} & \frac{\lambda}{2}I_1^2 + \mu I_2 - \gamma \int_{-\infty}^{\infty} w(\varepsilon_c) \\ & (I_1 - \varepsilon_c)\left[\sqrt{\left(\varepsilon_{nm} - \frac{1}{3}\varepsilon_c\delta_{nm}\right)\left(\varepsilon_{nm} - \frac{1}{3}\varepsilon_c\delta_{nm}\right)} \right. \\ & \left. - \frac{2}{\sqrt{3}}\sqrt{\varepsilon_c^2}\right] d\varepsilon_c \end{aligned} \qquad (17)$$

The last term, $\sqrt{\varepsilon_c^2}$, is added to meet the condition of zero stress for zero strain. With this energy form and using Eq. (1), the pressure-strain relations under hydrostatic conditions are:

$$P = -\frac{\sigma_{ii}}{3} = -\left(\lambda + \frac{2}{3}\mu\right) I_1 + \frac{2}{\sqrt{3}}\gamma \int_{-\infty}^{\infty} w(\varepsilon_c)\left[\sqrt{(\varepsilon_c - I_1)^2} - \sqrt{\varepsilon_c^2}\right] d\varepsilon_c. \quad (18)$$

Cracks closure under compressive stresses in Westerly granite samples was directly observed by Batzle *et al*. (1980). These observations include standard unheated samples and samples that were heavily cracked by cyclic heating up to 500°C. Their experiments demonstrated that at confining load below ~10 MPa and above ~40 MPa the stress–strain curves are linear, but with different slopes below and above these values (Fig. 3). Constant elastic moduli (blue lines in Fig. 3) are expected if the changes in the geometry (opening or closure) of the cracks are negligibly small, as assumed in models for the effective elastic properties of cracked solids (O'Connell and Budiansky, 1974; Budiansky and O'Connell, 1976; Kachanov, 1992). Transient behavior, associated with gradual closure of the initially opened cracks, occurs between ~10 and ~40 MPa (Fig. 3). As shown by the red lines in Fig. 3a, b, both sets of experimental results (from heated and unheated samples) are well fitted by Eq. (18). The employed weight function is:

$$w(\varepsilon_c) = \frac{1}{\sqrt{\pi}\Delta\varepsilon} \exp\left(-\frac{(\varepsilon_c - \varepsilon_0)^2}{\Delta\varepsilon^2}\right). \quad (19)$$

This form assumes that most of the randomly distributed cracks are closed under volumetric strain within the interval of strain values $\varepsilon_c = \varepsilon_0 \pm \Delta\varepsilon$. With $\Delta\varepsilon \to 0$, the weight function (Eq. 19) approaches the delta-function and the stress–strain curves have sharp crack closure at $\varepsilon = \varepsilon_c = \varepsilon_0$ (Eq. 15). Note that the experimental observations with unheated samples can also be fitted well with sharp crack closure (blue line in Fig. 3a). This significantly simplified formulation also provides a good fit to the experimental data with heated granite samples, excluding the range of strain values

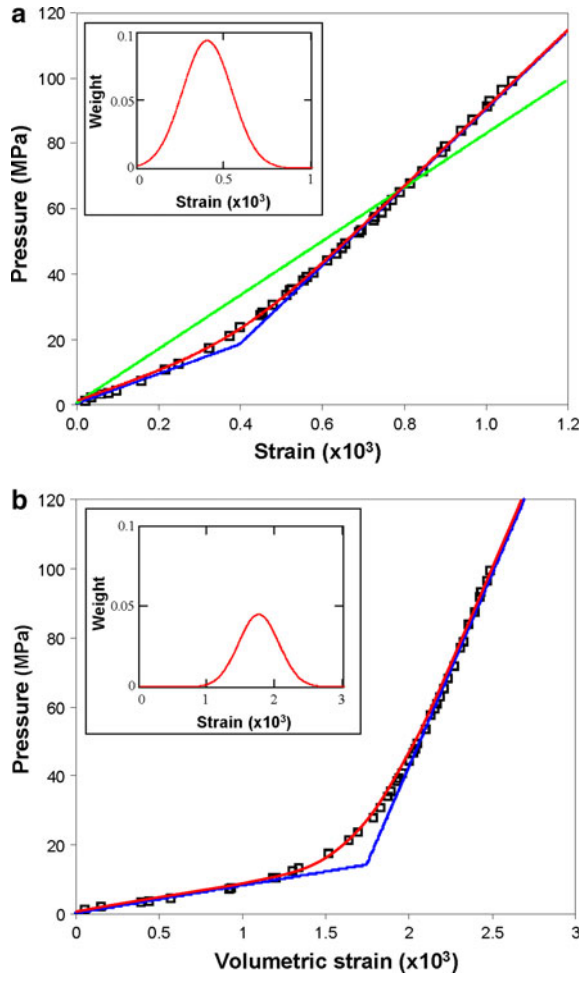

Figure 3
Measured pressure versus volumetric strain during hydrostatic loading experiments with Westerly granite (Batzle *et al*., 1980) compared with our model that accounts for crack closure. **a** Data obtained during experiments with unheated granite sample. **b** Data obtained during experiments with thermally cracked granite samples. The *blue line* indicates relations with sharp crack closure at ε_c (Eq. 15). The *red line* indicates gradual cracks closure around ε_c (Eq. 18) with weight shown in the *inset figures*. The *green line* in (**a**) gives the best fitted linear elastic model

where the gradual crack closure occurs. The modeled elastic moduli for the unheated samples (Fig. 3a) are $\lambda = \mu = 1.65 \times 10^4$ MPa and $\gamma = 0.65\mu$, which are slightly above the values used in the previous calculations. The Lame terms for the heated samples (Fig. 3b) are $\lambda = \mu = 1.2 \times 10^4$ MPa, which are the same as in the previous calculations, but the third (nonlinear) modulus, which is responsible for the different slopes in Fig. 3, is significantly larger,

$\gamma = 1.25 \times 10^4$ MPa. The parameters of the weight function are $\varepsilon_0 = 0.4 \times 10^{-3}$, $\Delta\varepsilon = 0.2 \times 10^{-3}$ for the unheated samples (Fig. 3a) and $\varepsilon_0 = 1.7 \times 10^{-3}$, $\Delta\varepsilon = 0.4 \times 10^{-3}$ for the heated samples (Fig. 3b). This means that, effectively, most crack closure occurs at strains between 0.2–0.6 $\times 10^{-3}$ for unheated samples and between 1.3–2.1 $\times 10^{-3}$ for heated samples. For strains well above those values, the shift in the location of the kink point may be neglected and taken as ε_0. In this case, which represents typical conditions for the seismogenic zone of the crust (not including some localities with very high pore pressure), the energy function of (Eq. 17) reduces back to that of (Eq. 4).

4. Discussion and Concluding Remarks

The strain energy function provides complete information on the stress–strain relations and effective elastic moduli of a deforming solid. In this study we focus on non-linear reversible deformation. Therefore, we do not consider any dissipative process that is associated with damage evolution, for example crack nucleation and growth or frictional sliding between crack faces. The strain energy of linear isotropic materials is associated with a second-order function of the strain tensor and two Lame coefficients. Beyond the early Hookean regime, different energy functions are appropriate for different classes of materials. In this paper we consider in detail two different models that can extend the linear Hookean regime to non-linear elastic behavior: the classical framework of Murnaghan (1951) and the presented non-classical model. The former framework includes analytical terms of all three strain invariants that are higher than second-order (Eq. 2) whereas the latter includes a non-analytical second-order term of the first two strain invariants (Eq. 4).

The Murnaghan model can produce gradual reduction of the slope of the stress–strain curve at relatively low stress levels, as observed in deformation of soft materials, for example graphite and soil (Kaji *et al*., 2001; Li and Ding, 2002). However, the Murnaghan model with the same values of coefficients cannot fit the extended linear regime of stiff rocks (Fig. 2a), nor does it explain the kink in observed stress–strain curves attributed to closure of initial cracks in such materials (Fig. 3). These two features can be modeled well by the non-analytical second-order potential (Eq. 4), and its extension developed in sect. "3.3". Another indication that the Murnaghan model can describe only a very limited deformation regime of stiff rocks is given by the fact that some of the third moduli estimated for Westerly granite by Johnson and Rasolofosaon (1996) and the fits of Fig. 1a are negative. This implies macroscopic weakening of the stress–strain curve and brittle failure (negative slope) at a stress level considerably below (Fig. 2a) that indicated by the observations.

The results associated with the non-analytical second-order energy potential (Eqs. 4–6 and Eq. 17 and 18) share some similarities with, and extend aspects of, other non-classical models, for example the clapping and unilateral damage models (Chaboche, 1992; Lamaitre and Desmorat, 2005; Pecorari and Solodov, 2006). These models address the observed bi-linear stress–strain relations for damaged stiff materials. Furthermore, our energy function produces dilation under shear loading, and can explain well various additional features observed in laboratory experiments with stiff rocks. These include the Kaiser effect (Hamiel *et al*., 2004), stress-induced anisotropy (Hamiel *et al*., 2009), and the asymmetric shape of resonance curves of damaged rocks and shift in the peak frequency with increasing excitation (Lyakhovsky *et al*., 2009). The developments of sect. "3.3" can account for gradual closure of different subsets of cracks with increased loading. The theoretical results fit well with a simple weight function (Eq. 19) the observations of Batzle *et al*. (1980) with unheated and thermally cracked granite samples. Using appropriate weight functions, the results can be used to model gradual closure of complex distributions of initial cracks in basalt and other heavily cracked materials (Stanchits *et al*., 2006). For normal stress levels appropriate for crustal depths larger than 1–3 km (under standard non-over-pressurized conditions), the existing cracks should be closed and the results of sect. "3.3" collapse to those associated with the energy function (Eq. 4).

We suggest that the non-analytical second-order energy function (Eq. 4) and associated results provide an appropriate quantitative framework for modeling

various non-linear features observed during deformation of stiff damaged rocks. For soft materials with strong curvature in the strain–stress relations during the elastic reversible regime the Murnaghan model provides an appropriate framework. We also recall that our simplified strain energy function (Eq. 4) depends only on I_1 and I_2, so the model may not account properly for situations where explicit incorporation of I_3 is needed. Such situations may be treated by Murnaghan model or the general second-order model (Eq. 10).

Acknowledgments

We thank the associate editor, Charles G. Sammis, and two anonymous reviewers for constructive reviews. The authors acknowledge support by the US–Israel Binational Science Foundation (BSF) grant number 2008248.

References

Alm, O., Jaktlund, L.L. and Kou, S. (1985), *The influence of microcrack density on the elastic and fracture mechanical properties of Stripa granite*, Phys. Earth Planet. Inter., *40*, 161–179.

Ambartsumyan, S.A. (1982), *Raznomodulnaya Teoria Uprugosti* (*a multimodulus elasticity theory*), Nauka, Moscow (in Russian).

Assimaki, D. and Kausel, E. (2002), *An equivalent linear algorithm with frequency- and pressure-dependent moduli and damping for the seismic analysis of deep sites*. Soil Dynamics and Earthquake Engineering, *22*, 959–965.

Bardet, J.P., Ichii, K. and Lin, C.H. (2000), EERA – A computer program for Equivalent-linear Earthquake site Response Analyses of Layered Soil Deposits. University of Southern California, Department of Civil Engineering.

Basaran, C. and Nie, S. (2004), *An irreversible thermodynamics theory for damage mechanics of solids*. Int. J. Damage Mach. *13*, 205–223.

Batzle, M.L., Simmons, G. and Siegfried, R.W. (1980), *Microcrack closure in rocks under stress: direct observation*, J. Geophys. Res., *85*(B12), 7072–7090, doi:10.1029/JB085iB12p07072.

Ben-Zion, Y. and V. Lyakhovsky (2006), *Analysis of Aftershocks in a Lithospheric Model with Seismogenic Zone Governed by Damage Rheology*, Geophys. J. Int., *165*, 197–210, doi: 10.1111/j.1365-246X.2006.02878.x.

Beresnev, I.A. (2002), *Nonlinearity at California generic soil sites from modeling recent strong-motion data*. Bull. Seismol. Soc. Am., *92*, 863–870, doi:10.1785/0120000263.

Birch, F. (1952), *Elasticity and constitution of the Earth's interior*, J. Geophys. Res, *57*, 221–286.

Bonner, B.P. (1974), *Shear wave birefringence in dilating granite*. Geophys. Res. Lett., *1*, 217–220.

Boness, N.L. and Zoback, M.D. (2006), *Mapping stress and structurally-controlled crustal shear velocity anisotropy in California*, Geology, *34*, 825–828.

Bonilla, L.F., Archuletta, R.J. and Lavallee, D. (2005), *Hysteretic and dilatant behavior of cohesionless soils and their effects on nonlinear site response: Field data observations and modeling*. Bull. Seismol. Soc. Am., *95*, 2273–2395, doi: 10.1785/0120040128.

Brace, W.F. (1965), *Some new measurements of the linear compressibility of rocks*, J. Geophys. Res. *70*, 391–398.

Brady, B.T., (1969), *The non-linear behavior of brittle rock*, Int. J. Rock Mech. Min. Sci. Geomech. Abstr. *6*, 301–310.

Budiansky, B. and O'Connell, R.J. (1976), *Elastic moduli of a cracked solid*. Int. J. Solids Struct., *12*, 81–97.

Chaboche, J. (1992), *Damage induced anisotropy: on the difficulties associated with the active/passive unilateral condition*. Int. J. Damage Mech., *1*, 148–171.

Christensen, R.M. (1979), *Mechanical of composite materials*, Wiley-interscience, New York.

Crampin, S. (1987), *Geological and industrial applications of extensive dilatancy anisotropy*, Nature, *328*, 491–496.

Exadaktylos, G.E. (2006), *Nonlinear rock mechanics*. In: (P.P. Delsanto, ed.) *Universality of nonclassical nonlinearity*, Springer, New York, p. 71–90.

Field, E.H., Johnson, P.A., Beresnev, I.A. and Zeng, Y., 1997. *Nonlinear ground-motion amplification by sediments during the 1994 Northridge earthquake*, Nature, *390*, 599–602.

Frankel, A.D., Carver, D.L. and Williams, R.A. (2002), *Nonlinear and linear site response and basin effects in Seattle for the M 6.8 Nisqually, Washington, earthquake*. Bull. Seismol. Soc. Am., *92*, 2090–2109. doi:10.1785/0120010254.

Gordon, R.B., and Davis L.A. (1968), *Velocity and attenuation of seismic waves in imperfectly elastic rocks*, J. Geophys. Res., *73*, 3917–3935.

Hall, S.A., Kendall, J.M., Maddock, J. and Fisher, Q. (2008), *Crack density tensor inversion for analysis of changes in rock frame architecture*, Geophys. J. Int. doi:10.1111/j.1365-246X.2008.03748.x.

Hamiel, Y., Liu, Y., Lyakhovsky, V., Ben-Zion, Y. and Lockner, D. (2004), *A visco-elastic damage model with applications to stable and unstable fracturing*, Geophys. J. Int., *159*, 1155–1165.

Hamiel, Y. Lyakhovsky, V., Stanchits, S., Dresen, G. and Ben-Zion, Y. (2009), *Brittle deformation and damage-induced seismic wave anisotropy in rocks*. Geophys. J. Int., *178*, 901–909.

Hatzell, S., Leeds, A., Frankel, A., Williams, R.A., Odum, J., Stephenson, W. and Silva, W. (2002), *Simulation of brad-band ground motion including nonlinear soil effects for a magnitude 6.5 earthquake on the Seattle fault, Seattle, Washington*. Bull. Seismol. Soc. Am., *92*, 831–853. doi:10.1785/0120010114.

Hatzell, S., Bonilla, L.F. and Williams, R.A. (2004), *Prediction of nonlinear soil effects*, Bull. Seismol. Soc. Am., *94*, 1609–1629, doi:10.1785/012003256.

Hughes, D.S. and Kelly, J.L. (1953), *Second-order elastic deformation of solids*, Phys. Rev., *92*, 1145–1149.

Johnson, P.A. and Rasolofosaon, P.N.J. (1996), *Nonlinear elasticity and stress-induced anisotropy in rock*, J. Geophys. Res. *101*, 3113–3124.

Johnson, P.A., Zinszner, B. and Rasolofosaon, P.N.J. (1996), *Resonance and elastic nonlinear phenomena in rock*, J. Geophys. Res. *101*, 11553–11564.

Johnson, P.A. (2006), *Nonequilibrium nonlinear-dynamics in solids: state of the art*. In: (P.P. Delsanto, ed.) *Universality of nonclassical nonlinearity*, Springer, New York, p. 49–69.

Jones, R.M. (1977), *Stress-strain relations for materials with different moduli in tension and compression*, AIAA J., *15*, 62–73.

Kachanov, M. (1992), *Effective elastic properties of cracked solids; critical review of some basic concepts*, Appl. Mech. Rev., *45*, 304–335.

Kaji Y., Gu W., Ishihara M., Arai T., and Nakamura H. (2001), *Development of structural analysis program for non-linear elasticity by continuum damage mechanics*, Nuclear Engineering and Design, *206*, 1–12.

Karageorgi, E., Clymer, R. and McEvilly, T.V. (1992), *Seismological studies at Parkfield. II. Search for temporal variations in wave propagation using Vibroseis*, Bull. Seism. Soc. Am. *82*, 1388–1415.

Lamaitre, J. and Desmorat, R. (2005), *Engineering damage mechanics*. Springer-Verlag, Berlin.

Leary, P.C., Crampin, S. and McEvilly, T.V. (1990), *Seismic fracture anisotropy in the Earth's crust: An overview*, J. Geophys. Res., *95*, 11,105–11,114.

Li, J. and Ding, D.W. (2002), *Nonlinear elastic behavior of fiber-reinforced soil under cyclic loading*, Soil Dynamics and Earthquake Engineering, *22*, 977–983.

Liu, Y., Teng, T.L. and Ben-Zion, Y. (2005), *Near-surface seismic anisotropy, attenuation and dispersion in the aftershock region of the 1999 Chi-Chi earthquake*, Geophys. J. Int., *160*(2), 695–706.

Lockner, D.A., Byerlee, J.D., Kuksenko, V., Ponomarev, A. and Sidorin, A. (1992), Observations of quasi-static fault growth from acoustic emissions. in Fault mechanics and transport properties of rocks, International Geophysics Series, Vol. 51, 3–31, eds Evans, B. and Wong, T.-f., Academic Press, San Diego, CA.

Lockner, D.A. and Byerlee, J.D. (1980), Development of fracture planes during creep in granite, in: H.R. Hardy, F.W. Leighton (Eds.), 2nd Conference on Acoustic Emission/Microseismic Activity in Geological Structures and Materials, Trans-Tech. Publications, Clausthal-Zellerfeld, Germany, pp. 1–25.

Lockner, D.A. and Stanchits, S.A. (2002), *Undrained poroelastic response of sandstones to deviatoric stress change*, J. Geophys. Res. *107*, doi:10.1029/2001JB001460.

Lyakhovsky, V., Hamiel, Y., Ampuero, P. and Ben-Zion, Y. (2009), *Nonlinear damage rheology and wave resonance in rocks*. Geophys. J. Int., *178*, 910–920.

Lyakhovsky, V. and Myasnikov, V.P. (1984), *On the behavior of elastic cracked solid*, Phys. Solid Earth, *10*, 71–75.

Lyakhovsky, V., Reches, Z., Weinberger, R. and Scott, T.E. (1997), *Non-linear elastic behavior of damaged rocks*, Geophys. J. Int., *130*, 157–166.

Miller, V. and Savage, M.K. (2001), *Changes in seismic anisotropy after volcanic eruptions: evidence from Mount Ruapehu*, Science, *293*, 2231–2233.

Murnaghan, F.D. (1951), *Finite deformation of an elastic solid*, John Wiley, Chapman, New York, 140 pp.

Nishihara, M. (1957), *Stress–strain relation of rocks*, Doshisha Eng. Rev. *8*, 32–54.

Nur, A. and Simmons, G. (1969), *Stress-induced velocity anisotropy in rock: An experimental study*, J. Geophys. Res., *74*, 6667–6674.

Nur, A. (1971), *Effects of stress on velocity anisotropy in rocks with cracks*, J. Geophys. Res., *76*, 2022–2034.

O'Connell, R.J., and Budiansky, B. (1974), *Seismic wave velocities in dry and saturated cracked solid*, J. Geophys. Res., *79*, 5412–5426.

Ogden, R.W. (1984), *Non-linear elastic deformations*. Dover Publications, New York.

Pasqualini, D., Heitmann, K., TenCate, J.A., Habib, S., Higdon, D. and Johnson, P.A. (2007), *Nonequilibrium and nonlinear dynamics in Berea and Fontainebleau sandstones: Low-strain regime*. J. Geophys. Res., *112*, B01204, doi:10.1029/2006JB004264.

Paterson, M.S. (1978), *Experimental Rock Deformation- the Brittle Field*, Springer-Verlag, Berlin.

Pavlenko, O.V. and Irikura, K. (2003), *Estimation of nonlinear time-dependent soil behavior in strong ground motion based on vertical array data*, Pure Appl. Geophys., *160*, 2365–2379.

Pecorari, C. and Solodov, I. (2006), *Nonclassical nonlinear dynamics of solid surfaces in partial contact for NDE applications*. In: (P.P. Delsanto, ed.) *Universality of nonclassical nonlinearity*, Springer, New York, p. 307–326.

Peng, Z. and Ben-Zion, Y. (2004), *Systematic analysis of crustal anisotropy along the Karadere-Duzce branch of the north Anatolian fault*, Geophys. J. Int., *159*, 253–274, doi: 10.1111/j.1365-246X.2004.02379.

Rathore, J.S., Fjaer, E., Holt, R.M., and Renlie, L. (1995), *P- and S-wave anisotropy of a synthetic sandstone with controlled crack geometry*, Geophys. Prosp., *43*, 711–728.

Reiner, M. (1945), *A mathematical theory of dilatancy*. Am. J. Math. *67*, 350–362.

Rubinstein, J.L. and Beroza, G.C. (2004), *Evidence for widespread nonlinear strong ground motion in the Mw 6.9 Loma Prieta Earthquake*, Bull. Seism. Soc. Am., *94*, 1595–1608.

Sammonds, P.R., Ayling, M.R., Meredith, P.G., Murrell, S.A.F., and Jones, C. (1989), A laboratory investigation of acoustic emission and elastic wave velocity changes during rock failure under triaxial stresses. In: Rock at great depth, eds: Maury, V., & Fourmaintraux, D., pp. 233–240, A.A. Balkema.

Sayers, C.M., van Munster, J.G., and King, M.S. (1990), *Stress-induced ultrasonic anisotropy in Berea sandstone*. Inter. J. Rock Mech., *27*, 4149–4156.

Schmitt, D.R. and Zoback, M.D. (1992), *Diminished pore pressure in low porosity crystalline rock under tensional failure: apparent strengthening by dilatancy*, J. Geophys. Res., *97,* 273–288.

Schock R.N. and Louis H. (1982), *Strain behavior of a granite and graywacke sandstone in tension*, Journal of Geophysical Research, *87*, 7817–7823.

Schock, R.N. (1977), The response of rocks to large stresses, in: D.L. Roddy, R.O. Pepin, R.B. Merrill (Eds.), Impact and Explosion Cratering, Pergamon Press, New York, pp. 657–688.

Sleep, N. H. and Hagin P. (2008), *Nonlinear attenuation and rock damage during strong seismic ground motions*, Geochem. Geophys. Geosyst., *9*, Q10015, doi:10.1029/2008GC002045.

Smith, E., and TenCate, J.A. (2000), *Sensitive determination of the nonlinear properties of Berea sandstone at low strains*, Geophys. Res. Lett., *27*, 1985–1988.

Solodov, I.Yu. and Korshak, B.A. (2002) *Instability, chaos, and "memory" in acoustic-wave – crack interaction*. Phys. Rev. Lett., *88*, 014303, doi:10.1103/PhysRevLett.88.014303.

Stanchits, S., Vinciguerra, S. and Dresen, G. (2006), *Ultrasonic velocities, acoustic emission characteristics and crack damage of basalt and granite*, Pure Appl. Geophys., *163*, 975–994.

TenCate J.A., Pasqualini D., Habib S., Heitmann K., Higdon D. and Johnson P.A. (2004), Nonlinear and Nonequilibrium Dynamics in Geomaterials. Phys. Rev. Lett., 93, 6, 065501

Truesdell, C. and Noll, W. (2004), The non-linear field theories of mechanics. 3ed., Edited by S.S. Antman, Springer-Verlag, Berlin, 627 pp.

Tsuda, K., Steidl, J., Archuleta, R. and Assimaki, D. (2006), *Site-response estimation for the 2003 Miyagi-Oki earthquake sequence consider nonlinear site response*. Bull. Seismol. Soc. Am., *96*, 1474–1482, doi:10.1785/0120050160.

Walsh, J.B. (1965), *The effect of cracks on the uniaxial elastic compression of rocks*, J. Geophys. Res. *70*, 399–411.

Weinberger, R., Reches, Z., Eidelman, A. and Scott, T.S. (1994), *Tensile properties of rocks in four-point beam tests under confining pressure*. In: P. Nelson, S.E. Laubach (Eds.), Proceedings First North American Rock Mechanics Symposium, Austin, Texas, pp. 435–442.

Winkler, K., Nur, A. and Gladwin, M. (1979), *Friction and seismic attenuation in rocks*, Nature, *277*, 528–531.

Wu, C., Peng, Z. and Ben-Zion, Y. (2009), *Non-linearity and temporal changes of fault zone site response associated with strong ground motion*, Geophys. J. Int., *176*, 265–278, doi: 10.1111/j.1365-246X.2008.04005.x.

Zamora, M. and Poirier, J.P. (1990), *Experimental study of acoustic anisotropy and birefringence in dry and saturated Fontainebleau sandstone*, Geophysics, *55*, 1455–1465.

Zoback, M.D. and Byerlee, J.D. (1975), *The effect of microcrack dilatancy on the permeability of Western granite*, J. Geophys. Res. *80*, 752–755.

(Received June 28, 2010, revised October 3, 2010, accepted November 16, 2010, Published online February 12, 2011)